Conformational Structures of 3-Phenyl-1-propionic Acid, Its *p*-Hydroxy Derivative, and Its Hydrated Clusters

John A. Dickinson, Paul W. Joireman, Robert W. Randall, Evan G. Robertson, and John P. Simons*

Physical and Theoretical Chemistry Laboratory, South Parks Road, Oxford OX1 3QZ, U.K.

Received: June 27, 1996; In Final Form: September 4, 1996[⊗]

We present fluorescence excitation and one- and two-color resonant two-photon ionization spectra of 3-phenyl-1-propionic acid (PPA), its complexes with water, $PPA(H_2O)_n$, where $n = 1-3$, and its *p*-hydroxy derivative, 3-(4-hydroxyphenyl)-1-propionic acid (HPPA), at the vibronic and partially resolved rovibronic level. Different conformations of the alkyl side chain in the bare molecule produce two spectral bands in the 0_0^0 region for PPA and three bands for HPPA. Analysis of the rovibronic band contours of these features is consistent with two conformational structures, referred to as anti and gauche. The anti structure is characterized by an extended side chain and a predominantly b-type band contour. The gauche structure is characterized by a side chain folded back toward the phenyl ring and a hybrid band contour. Analysis of this contour shows that there is a significant rotation of the transition moment within the molecular frame. Rovibronic band contour analysis of the 1:1 water complex of PPA yields a structure consistent with the acid acting as a proton donor. The rotational band contour of the 1:2 water complex is consistent with a cyclic structure in which each water is involved in two hydrogen bonds.

I. Introduction

Free jet expansion, coupled with laser induced fluorescence excitation (FE) or mass-selected, resonant two-photon ionization (MS-R2PI) spectroscopy, provides a powerful means of isolating and identifying distinct conformers of complex and solvated organic molecules in the gas phase.[1−7] Hole-burning or saturation spectroscopy can help in separating the contributions of individual components excited within the expansion,[1,2] while structural assignments can be made through analysis of rotationally resolved spectra in the frequency[4] or time domain.[5]

In the last few years, following the works of Levy,[1,2] Bernstein,[6] and Ito,[7] we have identified, assigned, and structurally characterized the conformers of a series of hydroxy- and amino-substituted benzoic acid esters.[4c] We have explored conformational preferences in a series of phenyl ethyl alcohols and amines.[4b] The interactions between the side chain and the ring are of particular interest in promoting folded (gauche) as opposed to extended (anti) molecular conformations. Most recently, we have investigated a series of phenylpropionic acids previously studied by Levy[2a] and Sulkes.[3] A new study of formanilide and its water clusters will be presented elsewhere.[8]

One of the prime motives for pursuing these experiments lies in their relevance to biomolecular systems. Protein chromophores such as phenylalanine, tyrosine, and tryptophan accommodate flexible side chains that can adopt different conformations with respect to the aromatic ring(s). Conformational preferences, reflected in the frequencies and intensities of their electronic spectra, may be influenced by both intramolecular interactions between the ring and the side chain and intermolecular interactions with bound solvent molecules, particularly water. Conformational choice may also influence the incidence of chemical processes such as proton or electron transfer. The transfer of a proton is a key step in many enzymatic reactions.

In this paper, we probe the conformational properties of 3-phenyl-1-propionic acid (PPA), a precursor of phenylalanine, its complexes with water, and its *p*-hydroxy derivative (HPPA), a precursor of tyrosine. The vibronic and partially resolved rovibronic spectra using both FE and one- and two-color mass-selected R2PI techniques have been recorded. Distinct conformations of the acid side chain have been identified and structurally characterized using rotational band contour analysis. Vibronic spectra of the water complexes reveal qualitatively different binding mechanisms for different conformations, while rovibronic spectra yield plausible structures which may be taken as first approximations pending higher resolution FE or R2PI spectra.

II. Experimental Section

A Nd:YAG laser (Spectron SL805; 1.1 W/355 nm, 10 Hz) was used to pump a grating-tuned dye laser (Lambda Physik FL2002, 15 mW/530 nm, 10 Hz), the doubled output of which served both as an excitation and photoionization laser in one-color R2PI experiments. Two-color experiments employed a second Nd:YAG-pumped and frequency-doubled dye laser (Spectra Physics GCR-11, 1.5 W/532 nm, 10 Hz, and PDL-3, 11 mW/585 nm) to provide the photoionization laser. The two doubled dye beam outputs were combined coaxially and directed into the interaction region of a differentially pumped time-of-flight mass spectrometer (R. M. Jordan, Co.),[9] at right angles to the expansion axis of a pulsed molecular beam (General Valve, Series 9, 800-μm orifice). Partially resolved rotational band contours were obtained by narrowing the bandwidth of the FL2002 pump laser to $\approx$0.08 using an intracavity etalon. Care was taken to avoid saturation of the $S_1 \leftarrow S_0$ transition. The two-color experiment was essential to achieving this, as the intensity of the etalon-narrowed excitation laser could be minimized while adjusting the intensity of the ionization laser in order to maintain the strength of the ion signal.

The samples were heated ($T = 120-140$ °C) and entrained in helium at a stagnation pressure of 3−4 bar. Water vapor was incorporated into the carrier gas by bubbling helium through a water sample held at room temperature in a bypass line equipped with a needle valve. Mass-resolved photoionization signals are sampled by a digitizing oscilloscope (Tektronix TDS 520) and recorded as a function of pump laser wavelength.

[⊗] Abstract published in *Advance ACS Abstracts,* December 15, 1996.

S1089-5639(96)01913-5 CCC: $14.00

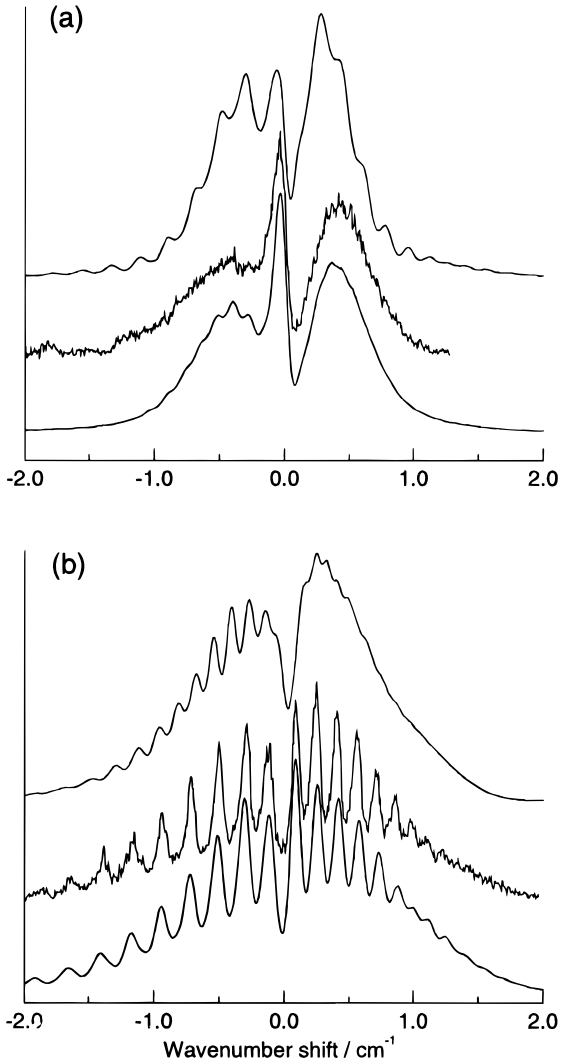

Figure 1. Rotational band contours of the two origin bands of PPA, determined by fluorescence excitation techniques, at (a) 37 649 and (b) 37 627 cm^{-1}. The experimental data are averaged over 10 laser shots, as are the other experimental spectra of PPA presented in this paper. These data lie above the best simulated band contour, the parameters of which are given in the text. The contour shown above each experimental spectrum is described in the text.

Partially resolved rotational band contours of the PPA monomer were obtained by fluorescence excitation experiments performed both at Oxford and at Prof. O. Kajimoto's laboratory in Kyoto. The Kyoto system consisted of an excimer-pumped, etalon-narrowed dye laser and pulsed molecular beam. The molecular beam conditions were similar to those described above. Fluorescence from the sample was detected by a photomultiplier (Hamamatsu R928), averaged by boxcar integrator (SRS 250) and recorded on a computer.

III. Results and Interpretation

III.A. 3-Phenyl-1-propionic Acid (PPA). Martinez *et al.*[2a] observed two closely spaced intense features, centered at 37 624 and 37 648 (close to the band-origin region of benzene[10a]), in the vibronically resolved FE spectrum of jet-cooled PPA. These were assigned as the origin bands of two conformers, one of which was tentatively associated with an anti conformation of the side chain. Figure 1 shows the partially resolved rotational band contours of each feature. Clearly, the species associated with the two bands have very different structures. R2PI spectra recorded at $m/e = 150$ confirm their assignment to PPA (*cf.* section III.C). The band contour of the feature we observe at 37 627 (note the slight difference between this value and the one in ref 2a) is shown in Figure 1b. It is predominantly b type, while the other feature is a hybrid band (Figure 1a) with a significant a component.

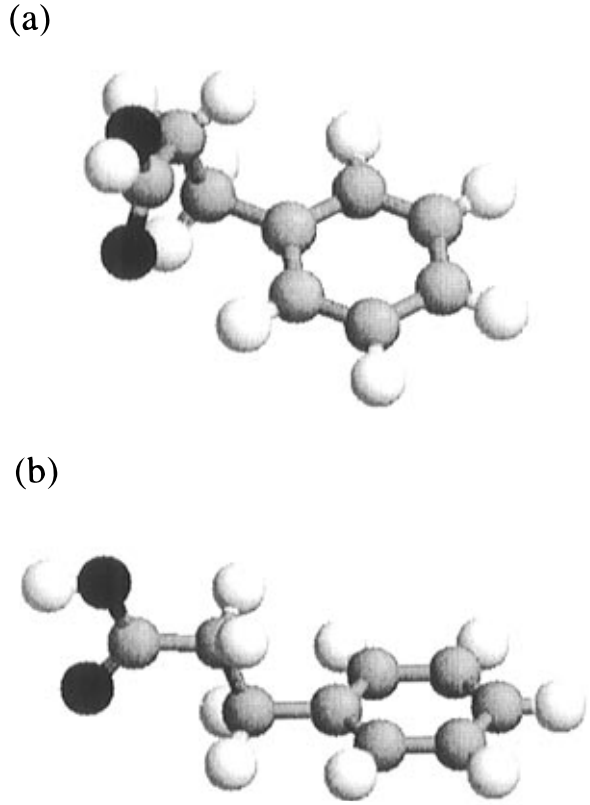

Figure 2. Structures consistent with the observed band contours of the PPA bands centered at (a) 37 649 cm^{-1} ($A'' = 0.0754$ cm^{-1}; $B'' = 0.0219$; $C'' = 0.0197$ cm^{-1}) and (b) 37 627 cm^{-1} ($A'' = 0.1102$ cm^{-1}; $B'' = 0.0152$ cm^{-1}; $C'' = 0.0148$ cm^{-1}). The structures are more fully described in section III.A.

Two side chain conformations, anti and gauche, are suggested by experimental and theoretical work on similar systems.[2a,6a,11,12] Models of the ground-state molecular structures, shown in Figure 2, were obtained from microwave structural data for toluene (ring geometry)[13] and ethylbenzene (side-chain bond lengths and angles).[14] Low-level ab initio calculations (anti, STO-3G basis; gauche, 3-21G basis) gave values for the side-chain torsional angles. The predicted ground-state rotational constants of each conformer are given in the caption to Figure 2.

In a rigid-rotor model, the appearance of any rovibronic band contour is additionally dependent on six parameters, $\Delta A = (A' - A'')/A''$, ΔB, ΔC, the band polarization, the temperature, and the experimental resolution. Electronic excitation of benzene results in an expansion of the ring, and translation of the predicted geometry changes[15] onto the PPA molecule leads to the expectations that $\Delta A = -3\%$, $\Delta B = -1\%$, and $\Delta C = -1\%$. (The negative values are qualitatively consistent with the experimentally observed red degradation of the band contours.) With these estimates, a series of band contour simulations involving iterative grid searches on each parameter was then performed.[4a] The two bands were initially assumed to be associated with a $\pi \rightarrow \pi^*$ transition polarized parallel to the short axis of the phenyl ring (*i.e.*, perpendicular to the axis directed along the $C-C_\alpha$ substituent bond), in conformity with the behavior observed for other monosubstituted benzenes.[16] The temperature and resolution were initially assumed to be 5 K and 0.08 cm^{-1}.

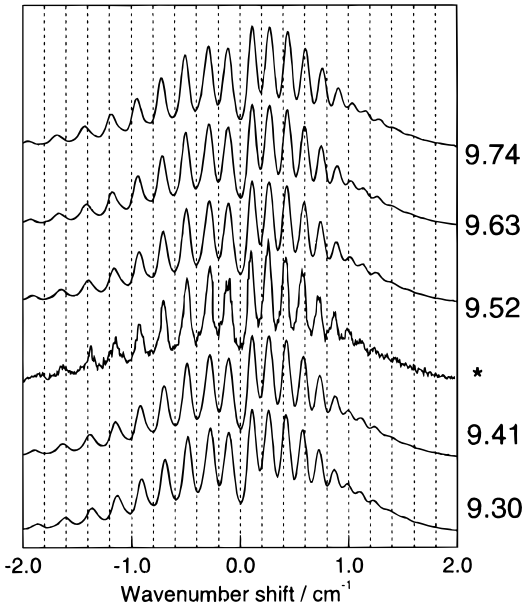

Figure 3. Rotational band contours calculated for different values of $A'' - \bar{B}''$, given next to each contour in units of 10^{-2} cm^{-1}, compared to the experimental spectrum (*) of the b-type band of PPA. The parameters used to calculate each contour are given in section III.A.

TABLE 1: Observed and Predicted Spectroscopic Constants of the Anti Conformer of PPA and Its Water Complexes

label	$A'' - \bar{B}''$/cm^{-1}	$B'' - C''/10^{-4}$ cm^{-1}
	PPA	
estd[a]	0.0938	≤10
pred[b] OH up[c]	0.0952	4
pred[b] OH down[c]	0.0977	5
	$PPA(H_2O)_1$	
estd[a]	0.0996	≤10
pred[b] site i OH up[c]	0.0724	1
pred[b] site i OH down[c]	0.0972	1
pred[b] site ii OH up[c]	0.1002	1
pred[b] site ii OH down[c]	0.0874	0.3
cyclic[d] site ii	0.0988	1
	$PPA(H_2O)_2$	
estd[a]	0.0667	≤5
pred[b] cyclic[e]	0.0675	1

[a] Refers to values calculated from the experimental data. [b] Refers to values calculated from the assumed ground-state molecular structure which is described in the text and shown in Figure 2b for PPA and Figure 10 for its water clusters. [c] Refers to different values of the $C_\alpha-C_\beta-C_\gamma-O$ dihedral angle ϕ; $\phi = 0$ for "OH up" (*cf.* Figure 2b); $\phi = 180$ for "OH down". [d] In this structure, the water acts as a proton acceptor from the carboxyl hydrogen and proton donor to the carbonyl oxygen following ref. 18. [e] Refers to a structure, shown in Figure 10b, in which both water molecules are involved in two hydrogen bonds.

III.A.1. PPA Anti Conformer. Polarization along the short axis when taken together with the 2-fold symmetry of the anti conformer strongly suggests the assignment of the b-type band at 37 627 to this conformer. Grid searches implemented on all the parameters using the calculated anti rotational constants converged to the values $\Delta A = -4\%$, $\Delta B = 0\%$, and $\Delta C = -1\%$, 100% b-type polarization, $T = 4 \pm 1$ K, and 0.08-cm^{-1} resolution. A band contour calculated using these values is compared to the experimental data in Figure 1b. Despite some minor differences between the two, specifically a slight mismatch in the intensities of some subbands and a small difference in the ^rQ band positions (which can be accommodated by reducing the value of A'' by 1%), the assignment of the b-type band to the anti conformer is confirmed. A band contour calculated using the ground-state rotational constants for the gauche conformer, using similar values for ΔA, ΔB, ΔC, and a short axis polarized transition moment (TM), is also shown in Figure 1b for comparison.

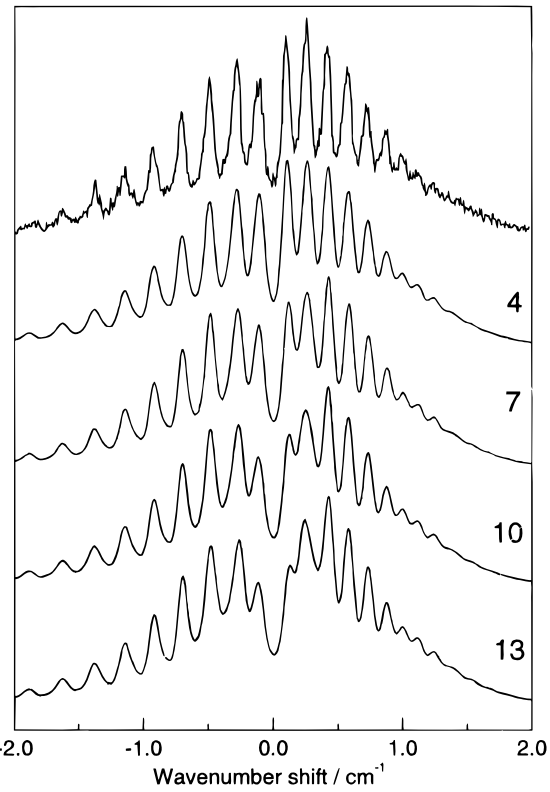

Figure 4. Rotational band contours calculated for different values of $B'' - C''$, given next to each contour in units of 10^{-4} cm^{-1}, compared to the experimental spectrum (top) of the b-type band of PPA. The value of $A'' - \bar{B}''$ was fixed at 0.0941 cm^{-1} to obtain the best possible match between the *Q* subband head positions. Additional parameters used to calculate each contour are described in section III.A.

We provide two further examples of the sensitivity of the anti band contour to the input parameters. The spacing of the *Q* subband heads is sensitive to the value of $A'' - \bar{B}''$, where $\bar{B}'' = {}^1/_2(B'' + C'')$. $A'' - \bar{B}''$ may be estimated from the experimental spectrum, using combination differences between appropriate subband heads, as 0.0938. Figure 3 shows a series of simulations at different values of $A'' - \bar{B}''$. The value of A'' has been changed by ±1−2%, with $\bar{B}''$ being fixed at 0.015 cm^{-1} since the value of $A'' - \bar{B}''$ is essentially controlled by the value of A''. The positions of the subband heads change slightly as a result of these changes. The best match to the experimental positions is obtained when $A'' - \bar{B}'' = 0.0941$ cm^{-1}, which compares well with the estimated value. Clear differences in position are observed for changes in $A'' > \pm 2\%$. The values of $A'' - \bar{B}''$ obtained here and those for the modeled structure are given in Table 1 for comparison. The value of $A'' - \bar{B}''$ for an alternate geometry in which the C_α-C_β-Cγ-O dihedral angle is rotated by 180° ("OH down") is also given in Table 1. This value is larger than both the estimated value and that for the "OH up" partner. Thus, the OH up form of the anti conformer gives a better fit to the experimental data.

In addition to information about $A'' - \bar{B}''$, the appearance of the experimental spectrum is sensitive to the value of $B'' - C''$, the asymmetry of the molecule. This is shown in Figure 4, where a series of simulations calculated at different values of $B'' - C''$ are compared to the experimental curve. It is clear that values of $B'' - C'' > 0.0010$ cm^{-1} (30 MHz) are inconsistent with the experimental data.

III.A.2. PPA Gauche Conformer. The band contour shown at the top of Figure 1b is the contour calculated using the assumed gauche structure (Figure 2a) and a short-axis-polarized TM. Clearly, it bears no resemblance to either experimental spectrum. All attempts to simulate the hybrid contour (*cf.* Figure 1a) using grid searches which retained the TM alignment parallel to the short axis of the phenyl ring were unsuccessful. An acceptable simulation of the hybrid band was only possible by allowing the TM alignment to rotate in the molecular frame. The grid searches conducted under this condition converged to the parameter values $\Delta A = -2\%$, $\Delta B = -1\%$, and $\Delta C = 0\%$, an a:b:c hybrid composition of 6−7:3−2:1, $T = 4 \pm 1$ K, and a resolution of 0.08 cm^{-1}. The resulting simulated band contour is shown at the bottom of Figure 1a. A simulation using the assumed anti structure and a hybrid composition of 7:2:1 is shown at the top of Figure 1a.

The high degree of a-type character cannot be attributed to inertial axis rotation alone. Instead, it must reflect an additional rotation of the transition moment of at least 30° toward the *a* axis, arising from a perturbation of the electronic transition in the gauche conformer.[4c] Such a perturbation may be associated with an interaction between the polar side chain and the aromatic π-electron system or may be the result of symmetry breaking due to rotation of the side chain away from the anti structure.

III.B. 3-(*p*-Hydroxyphenyl)-1-propionic Acid (HPPA). Martinez *et al.*[2a] and Teh and Sulkes[3b] have both recorded a vibronically resolved LIF spectrum of the *p*-hydroxy-substituted PPA (HPPA). The two spectra are virtually identical, with three strong features in the band-origin region centered at 35 566, 35 716, and 35 735 cm^{-1}. Martinez *et al.* concluded on the basis of a saturation experiment that only one conformer was stabilized in the jet expansion. The most intense band at 35 566 cm^{-1} was tentatively assigned as the origin of an anti conformer. The two other bands were tentatively assigned to side-chain torsional modes. Teh and Sulkes, however, concluded that the three features were not vibronically related on the basis of a comparison between the low-frequency vibronic structure in the dispersed fluorescence spectrum of each peak. Figure 5, which shows the partially resolved rotational band contours of each band, provides strong support for the latter conclusion. The single band we observe at 35 565 cm^{-1} exhibits a predominantly b-type contour, while the other two bands are both strongly hybridized, though their structures are not identical. Qualitatively, there are strong similarities between the b-type and hybrid bands in HPPA and the anti and gauche conformers in PPA.

Rotational band contour simulations provide further evidence. Estimates of the ground-state rotational constants of HPPA were obtained in a similar fashion to PPA as described above. Ground-state constants of the anti conformer were predicted to be $A'' = 0.1055$, $B'' = 0.011\,43$, and $C'' = 0.011\,24$ cm^{-1}. Upper-state rotational constants were predicted by considering the bond-length changes which would reproduce the observed ΔA, ΔB, and ΔC values in 4-ethylphenol[2c] (*e.g.*, the C−O distance decreases by 0.2 Å, the C_2-C_3 and C_5-C_6 distances increase by 0.014 Å, and other ring C−C distances increase by 0.06 Å). This gave estimated changes in *A*, *B*, and *C* upon excitation of −4%, 0%, and 0%, respectively. Ground-state rotational constants for the gauche structures were predicted to be 0.0666, 0.016 17, and 0.014 76 cm^{-1}, with changes upon excitation of −2%, 0%, and 0%, respectively. From inertial considerations alone, the band hybridization is calculated to be 8:74:18.

III.B.1. HPPA Anti Conformer. The variation of band contours with temperature provides additional information. For this reason, the band contours discussed below were recorded at different distances between the laser beam and the nozzle in order to vary the effective rotational temperature. b-Type band simulations using these parameters nearly match the band contours of the vibronic feature at 35 565 cm^{-1}, shown in Figure 5a. The slight discrepancy in *Q*-branch positions can be eliminated by using $A'' = 0.1040$ cm^{-1} ($A'' - \bar{B}'' = 0.0927$ cm^{-1}) and $\Delta A = -5\%$, as in the simulations shown. Although the magnitude of $\bar{B}''$ cannot be determined at the present resolution, some information can be gained about $B'' - C''$. Simulations were carried out in which the value of $B'' - C''$ was varied in a similar fashion to PPA. Only those with $0.000\,10 < B'' - C'' < 0.000\,30$ cm^{-1} reproduced the observed

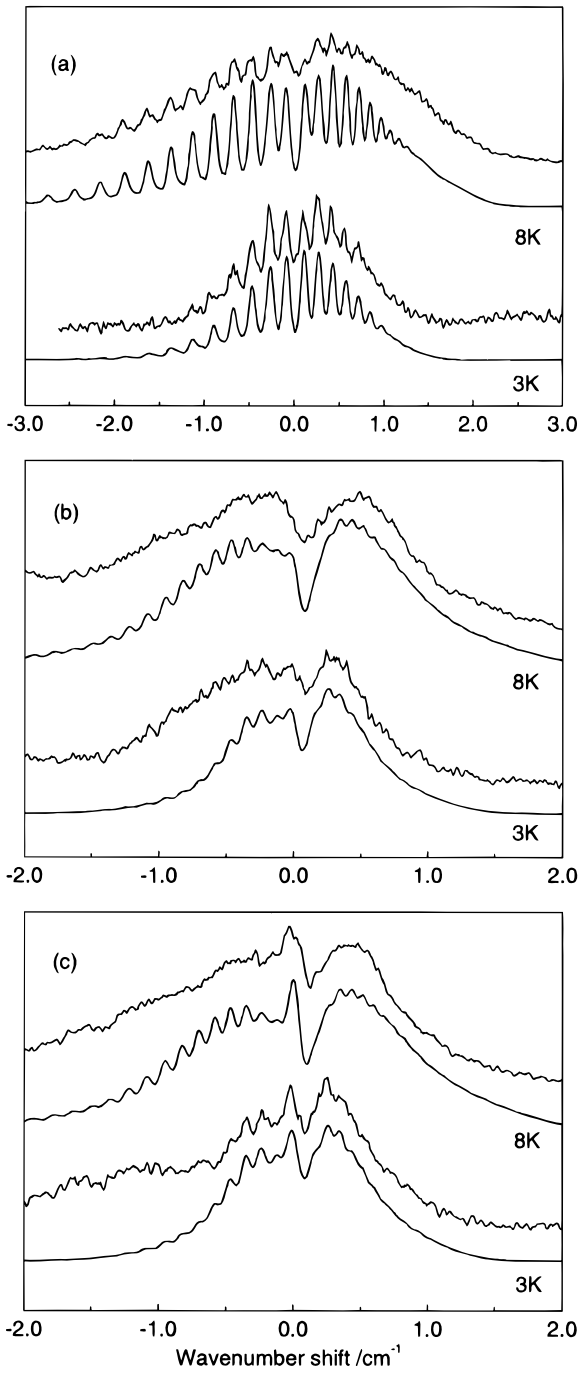

Figure 5. Rotational band contours of the HPPA bands at (a) 33 565, (b) 33 715, and (c) 33 733 cm^{-1}. Two simulations are shown for each band, recorded at different rotational temperatures as described in the text. The experimental data are averaged over 40 laser shots. The band contour simulations lie below the experimental spectra. The parameters used to calculate each contour are fully described in section III.B.

TABLE 2: Observed and Predicted Spectroscopic Constants of HPPA

label	$A'' - \bar{B}''/\text{cm}^{-1}$	$B'' - C''/10^{-4}\ \text{cm}^{-1}$
	Anti	
est[a]	0.0927(20)	1−3
pred[b] OH up[c]	0.0942	1.9
pred[b] OH down[c]	0.0974	2.3
X-ray structure[15]	0.0967	1.8
planar[d]	0.0976	11
	Gauche	
estd[a]	0.05(1)	−
pred[b]	0.0511	14

[a] Refers to the value estimated from the experimental spectrum. The value estimated for the gauche isomer is identical for the bands at 35 715 and 35 733 cm^{-1}. [b] Refers to values calculated from the assumed ground-state molecular structures discussed in the text. [c] Refers to different values of the $C_\alpha-C_\beta-C_\gamma-O$ dihedral angle ϕ; $\phi = 0$ for "OH up" (*cf.* Figure 2b); $\phi = 180$ for "OH down". [d] Refers to a geometry in which the heavy atoms of the side chain lie in the plane of the phenyl ring.

positions and intensities of the *Q* branches with low values of K_a. The higher temperature spectrum was more sensitive in this regard. (The structure in the higher temperature spectrum is not as well resolved as the corresponding simulation would suggest, possibly due to underlying hot bands or partial saturation.) The information obtained about $A'' - \bar{B}''$ and $B'' - C''$, shown in Table 2, together with the fact that the peak at 35 565 cm^{-1} is not present as a doublet, strongly points toward its assignment to the anti conformer. The X-ray crystal structure of HPPA[11] exhibits an anti conformation with a calculated $A'' - \bar{B}''$ value somewhat greater than the observed value for the gas phase. A structure in which the carbon atoms of the side chain lie in the plane of the phenyl ring gives a value of $A'' - \bar{B}'' = 0.0976\ \text{cm}^{-1}$, which is similar to the predicted value of the anti structure, but a much larger value for $B'' - C'' = 0.0011\ \text{cm}^{-1}$ when compared to the predicted anti value.

III.B.2. HPPA Gauche Conformers. Band contours of the pair of bands we observe at 35 715 and 35 733 cm^{-1} are shown in Figure 5b and 5c, respectively. There is just sufficient structure in the bands to estimate roughly the size of $A'' - \bar{B}''$ as *ca.* 0.05 cm^{-1}. This is consistent with the predicted value of 0.051 cm^{-1}. The calculated hybrid ratio, however, does not adequately reproduce the observed profiles of these two bands. In particular, more a-type character is required. The simulations shown in Figure 5b,c use the ratios 30:60:10 and 25:50:25 for the bands at 35 715 and 35 733 cm^{-1}, respectively. These estimates were obtained by grid searches as described earlier and comparison of both the cool (3 K) and slightly warmer (*ca.* 8 K) spectra. The differences in structure of these bands is more apparent in the higher temperature spectra. The variation of these band contours with temperature thus provides some additional information and helps, for example, in distinguishing a-type and c-type contributions.

Apart from inertial considerations, there are two electronic effects which may contribute to a rotation of the transition dipole moment. The orientation of the lone pair on the phenolic oxygen may affect the electron distribution. In *m*-cresol, flipping the H on the oxygen rotates the transition moment by *ca.* 12°.[4c] While this may account for the difference between the two gauche bands, it does not fully explain the amount of a-type character which is observed. An interaction between the chain and the ring, such as we propose for the gauche conformer of PPA, may be responsible, though the effect is less pronounced in HPPA than in PPA.

III.C. Water Clusters. Figure 6 shows a series of one-color mass-selected R2PI spectra of PPA in a water-seeded He expansion. These excitation spectra were recorded for each of the mass channels corresponding to $PPA(H_2O)_n$, $n = 0-3$. Features in addition to the monomer band origins are assigned to water clusters of PPA as designated in the figure. Extended scans, 300 cm^{-1} to the red or blue of the two band origins, did not reveal any additional spectral features attributable to water clusters. The one-color R2PI spectra displayed in Figure 6 reveal extensive fragmentation of the cluster ions, leading to contamination of the spectra recorded for the lower mass channels. In order to minimize the amount of fragmentation and facilitate band assignments, two-color mass-selected R2PI spectra were also recorded. These allowed ionization at a lower total energy ($\lambda_{\text{probe}} = 292.5$ nm); the results are shown in Figure 7.

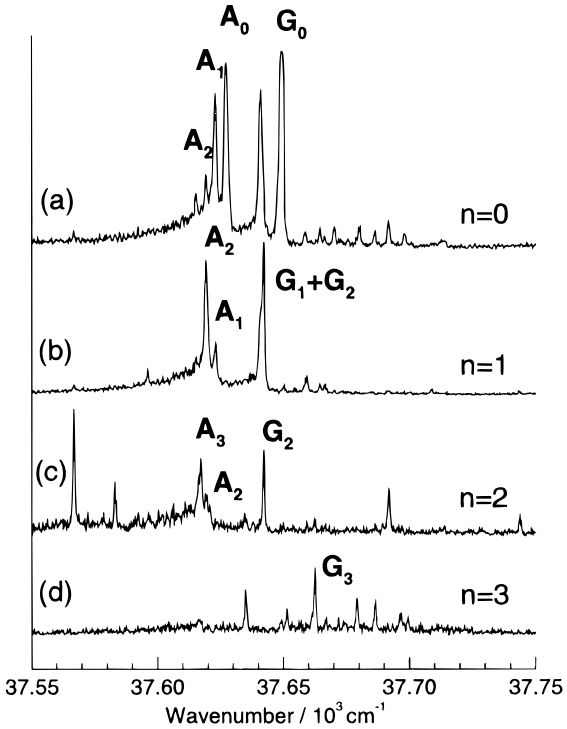

Figure 6. One-color R2PI spectra recorded at the (a) PPA, (b) $PPA(H_2O)_1$, (c) $PPA(H_2O)_2$, and (d) $PPA(H_2O)_3$ mass channels. The spectra in c and d were scaled up by a factor of 4. The labels $\mathbf{A}_n$ and $\mathbf{G}_n$ denote those bands assigned to complexes of the A or G conformer and *n* water molecules. The band positions are given in Table 3.

Comparisons between Figure 6 and Figure 7 are revealing. The most intense cluster bands in Figure 6b ($n = 1$) are due to clusters with $n = 2$; similarly, the most intense cluster bands in Figure 6c ($n = 2$) arise from fragmentation of ions with $n = 3$. In contrast, the most intense bands in the corresponding two-color spectra, shown in Figure 7b and 7c, correspond to those associated with the selected mass channel, confirming the suppression of cluster ion fragmentation at energies close to the ionization threshold. Stoichiometric assignments based upon the one- and two-color mass-selected R2PI spectra are summarized in Table 3.[17] The reduced intensity of the anti origin band in the two-color R2PI spectrum is real and reflects the different ionization potentials of the two conformers; 71 727 ± 50 cm^{-1} (anti) and 71 039 ± 50 cm^{-1} (gauche).

The question now arises as to the structure of the hydrated clusters and the degree to which the host molecular conformations are perturbed by cluster formation. Assignments based solely upon vibronic spectra do not allow the association of an individual cluster band with a particular monomer origin. This question can only be addressed by recording the spectra at higher resolution. Figures 8 and 9 show rovibronic band contours of the $PPA(H_2O)_n$ features with $n \leq 2$ which lie close to the bare

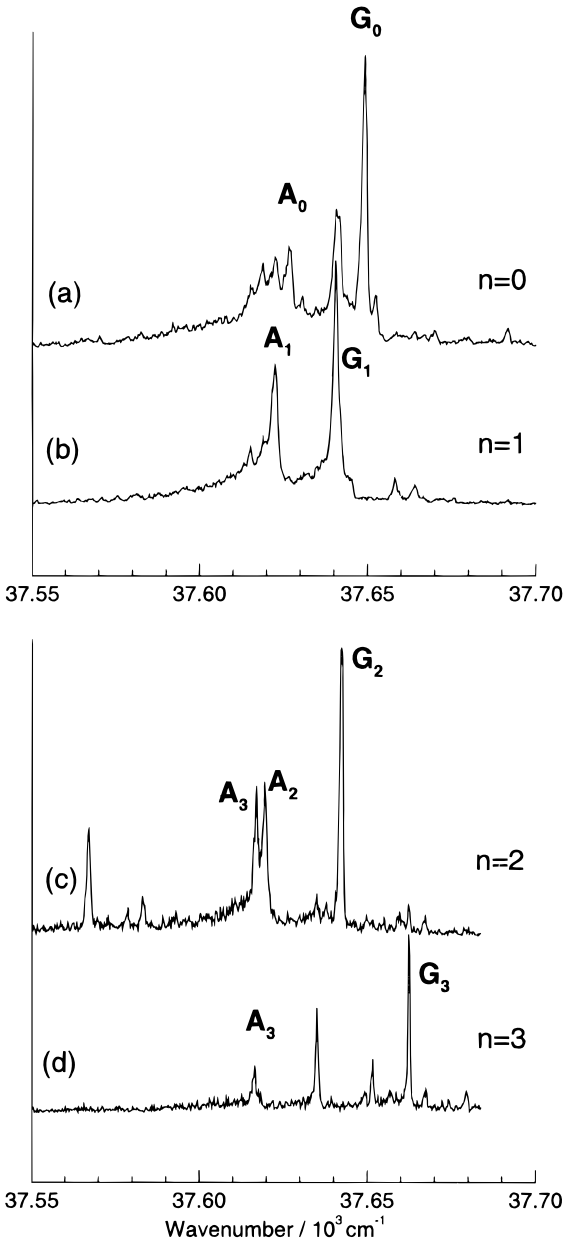

Figure 7. Two-color R2PI spectra recorded at the (a) PPA,(b) PPA-$(H_2O)_1$, (c) PPA$(H_2O)_2$, and (d) PPA$(H_2O)_3$ mass channels. The labels are the same as those used in Figure 6.

TABLE 3: Transition Wavenumbers for 3-Phenyl-1-propionic Acid (PPA) and Its Water Complexes

	conformer A		conformer G	
species	$\bar{\nu}$/cm^{-1}	$\delta\bar{\nu}$/cm^{-1}	ν/cm^{-1}	$\delta\bar{\nu}$/cm^{-1}
PPA	37 627		37 649	
PPA$(H_2O)_1$	37 623	−5	37 641	−8
PPA$(H_2O)_2$	37 619	−8	37 642	−7
PPA$(H_2O)_3$	37 617	−10	37 662	+13

molecule origin bands. The two bands displaced 5 and 8 cm^{-1} to the red of the anti conformer origin and associated with 1:1 and 1:2 water clusters have a similar appearance to the anti monomer origin. In a similar way, those lying 10 and 8 cm^{-1} to the red and 13 cm^{-1} (not shown) to the blue of the gauche conformer continue to display similarly hybridized, predominantly *a*-type profiles. Their assignment to the 1:1 and 1:2 hydration clusters of the anti and the 1:1, 1:2, and 1:3 clusters of the gauche molecular conformers, respectively, is strongly suggested. The blue shift associated with the 1:3 band (G_3) could arise through interaction of one of the bound water

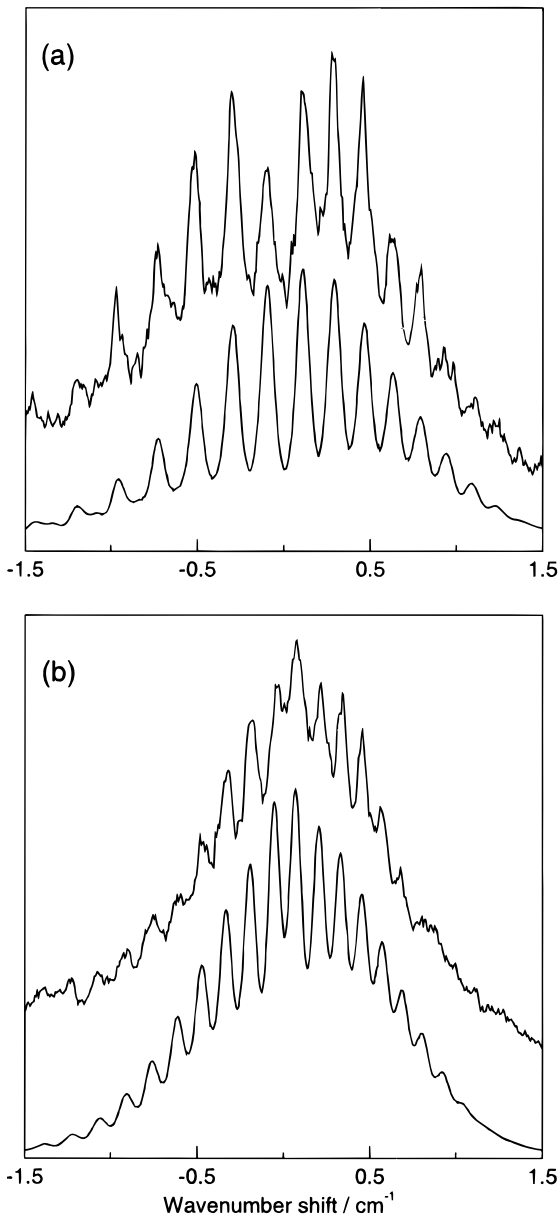

Figure 8. Rotational band contours from R2PI for the PPA−water complexes associated with the anti conformer of PPA: (a) PPA$(H_2O)_1$ and (b) PPA$(H_2O)_2$. The experimental data lie above the best simulated rotational band contour. The parameters used in each simulation are (a) $\Delta A = -4\%$, $\Delta B = 0\%$, $\Delta C = -1\%$, $T = 3$ K, 100% b type and (b) $\Delta A = -3\%$, $\Delta B = 0\%$, $\Delta C = 0\%$, $T = 2.5$ K, 100% *c* type. The predicted structures are described in the text and shown in Figure 10.

molecules with the aromatic ring. The band displaced 10 cm^{-1} to the red of the anti conformer origin is tentatively assigned as the 1:3 complex of this conformer, pending an analysis of its rovibronic structure. Finally, there are two further 1:3 cluster features lying between the peaks labeled A_3 and G_3 (Figure 7d) and a third lying slightly to the blue of G_3. These features are from a regular progression, based on A_3, with a spacing of 16−17 cm^{-1}. In the absence of higher resolution data, however, further speculation as to their assignment is unwarranted.

On the basis of these observations, a series of band contour simulations was conducted, assuming the retention of the host molecular geometry within each of its hydrated clusters. Again we used the observed monomer band polarizations as a starting point and standard hydrogen bond lengths as an initial guide to cluster dimensions. Three possible binding sites were investigated: (i) hydrogen bonding by proton donation to the carbonyl group, (ii) hydrogen bonding by proton acceptance from the

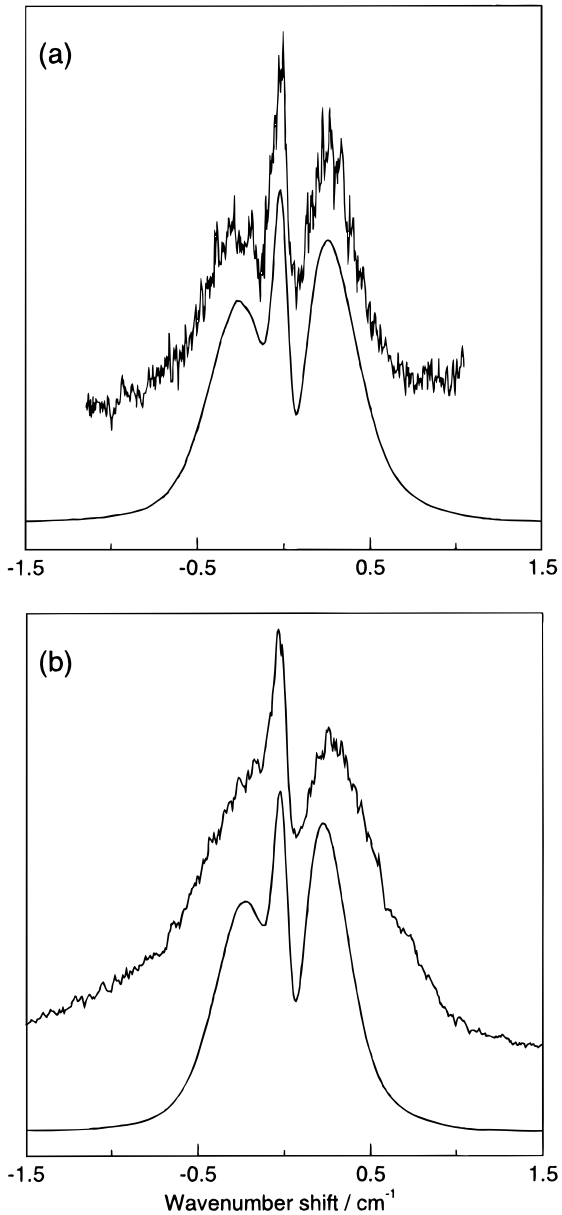

Figure 9. Rotational band contours for the PPA−water complexes associated with the gauche conformer of PPA: (a) $PPA(H_2O)_1$ from FE and (b) $PPA(H_2O)_2$ from R2PI. The experimental data lie above a simulated rotational band contour.

carboxyl hydrogen, and (iii) bonding *via* the π-electron system above the plane of the aromatic ring. Binding site iii is least likely given the small spectral shifts[10b] and did not lead to acceptable simulations of the experimental spectra.

III.C.1. *anti*-PPA−Water Complexes. Figure 8 shows the partially resolved band contours and optimized simulations for the 1:1 and 1:2 clusters of the anti conformer. The *Q* subband spacings in the 1:1 and 1:2 clusters are, respectively, more and less widely spaced than those in the host molecular conformer. An increased spacing implies an increase in $A'' - \bar{B}''$ and binding to the carboxylic hydrogen, site ii, which places the H_2O molecule close to the a inertial axis and far from the b axis. Similarly, a decreased spacing requires a decrease in $A'' - \bar{B}''$. Addition of the second water molecule through H-bonding to the carbonyl group, site i, would introduce a change in this direction. The values of $A'' - \bar{B}''$ were estimated from the experiment along with the values associated with various structures. These are summarized in Table 1 for both the 1:1 and 1:2 clusters. In addition, a limiting value of $B'' - C''$ was estimated in a similar way to that described in section III.A.1.

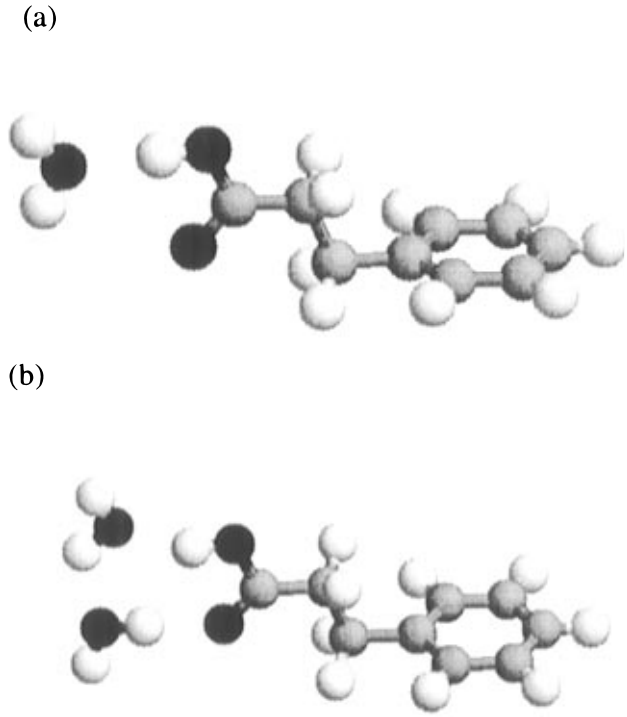

Figure 10. Molecular structures for the (a) $PPA(H_2O)_1$, R(O···O) 2.90 Å, linear hydrogen bond ($A'' = 0.1092$, $B'' = 0.094$, $C'' = 0.0093$ cm^{-1}), and (b) $PPA(H_2O)_2$, R(O···O) 2.75 Å ($A'' = 0.0745$, $B'' = 0.0074$, $C'' = 0.0073$ cm^{-1}), complexes of the anti conformer. The heavy atom(s) of the water adduct(s) lies in the same plane as the heavy atoms of the COOH group. Similar structures were used to model the gauche conformer.

The optimized simulations, Figure 8, and the corresponding cluster structures support both of these qualitative inferences. Thus, the general structure of the 1:1 complex is one in which the water binds as a proton acceptor at site ii.

Two structures consistent with the general 1:1 structure were investigated, a linear hydrogen-bonded geometry, shown in Figure 10a, and a cyclic geometry (not shown), in which the water acts as a proton acceptor to site ii and a proton donor to site i.[18] Both structures give rotational constants (given in Table 1) that fit the experimental spectrum reasonably well. Thus, the difference between these two geometries cannot be distinguished at this level of resolution. The contour is insensitive to the hydrogen bond length, since the O atom is simply being moved along the *a* axis in a linear hydrogen-bonded structure and no bounds could be placed on its value. However, the acceptable angular deviation from a linear hydrogen bond decreases with increasing hydrogen bond length. If the hydrogen bond distance is fixed at 2.9 Å, the allowable angular deviation from a linear hydrogen bond is $\leq 10°$.

The 1:2 complex was assumed to bound in a cyclic structure,[19] shown in Figure 10b, where the water heavy atoms are in the plane of the carboxyl group. The hydrogen bond length was taken as 2.75 Å between heavy atoms, and the bond angles were adjusted to accommodate this. The rotational constants of this structure describe a highly prolate symmetric top ($\kappa = -0.996$) in which the *b* and *c* axes have switched. The *c* axis is now parallel to the short axis of the phenyl ring and, assuming this polarization (perpendicular-type transition in the prolate limit), gives rise to the simulation shown in Figure 8b.

III.C.2. *gauche*-PPA−Water Complexes. Figure 9a,b shows the partially resolved rovibronic band contours from FE ($PPA(H_2O)_1$) and R2PI ($PPA(H_2O)_2$) for the 1:1 and 1:2 clusters of the gauche isomer. Band contour simulation for the gauche molecular clusters presents a much greater degree of difficulty

at the current level of spectral resolution. Thus, extensive simulations were not attempted. For the 1:1 complex, we assumed a linear and cyclic hydrogen-bonded structure, with initial binding to site i. The rotational constants consistent with this structure and a band polarization similar to that used for the monomer reproduce the observed band contour reasonably well, as shown in Figure 9a. The projections of the transition moment onto the inertial frame will change with the addition of the water molecule, but this change will favor a larger a component as the *a* axis will rotate toward the short axis of the phenyl ring. The 1:2 complex geometry was assumed to retain the cyclic geometry discussed above for the 1:2 complex of the anti isomer. A band contour simulation using these rotational constants is shown below the experimental contour in Figure 9b. No attempt at optimization was made.

IV. Discussion and Conclusions

IV.A. Isolated Molecular Conformers. The results of the band contour simulations of the origin bands of PPA and HPPA have enabled the determination of their conformational structures. Two side-chain conformers have been observed. The anti conformer exhibits a side chain extended away from the aromatic ring (*cf.* Figure 2b), while in the gauche conformer the side chain is folded back toward the aromatic ring (*cf.* Figure 2a). In HPPA, two vibronic bands (35 715 and 35 733 cm^{-1}) give rovibronic contours consistent with the gauche conformation. This can be attributed to the alternative orientations, cis or trans, of the phenolic OH with respect to the side chain. Band contours for the anti conformers may be simulated using a predominantly b-type transition, indicating that the transition moment is aligned approximately parallel to the short axis of the aromatic ring. In contrast, simulations of the band contours associated with the gauche conformers display strongly hybridized characters. The considerable a-type character of these bands cannot be accommodated by the inertial axis rotation introduced by the conformational change. An additional rotation of the transition dipole in the molecular frame is required, estimated to be 40° for PPA. The equivalent angle for HPPA is 15 ± 5°, modulated by the cis−trans orientation of the OH group.[4c] The reduced rotation angle in HPPA could reflect an opposing contribution from the OH substituent or a less folded side-chain conformation.

Fully optimized ab initio calculations (RHF; 6-31G*), which have explored the conformational landscape of PPA,[20] provide further support for our results. The calculations predict nine conformers, only four of which have appreciable population at room temperature. The global minimum has a calculated structure virtually identical to that of the anti conformer with a relative population of 54% at room temperature. The conformer lying closest in energy to the global minimum, with a relative population of 31% at room temperature, has a structure very similar to that of the gauche conformer (*cf.* Figure 2a). At the nozzle temperature of 413 K, the population ratio of the anti-to-gauche conformer is predicted to be 1:0.69. The relative vibronic band intensities as reported by Martinez *et al.*[2a] are close to this ratio; however, the vibronic spectra reported herein are not. In this work, the gauche band displays a slightly greater intensity than the anti band in the FE (not shown) and one-color R2PI spectrum (*cf.* Figure 6) and a markedly greater intensity in the two-color R2PI spectrum (*cf.* Figure 7). The discrepancy in the FE and one-color R2PI spectrum may reflect a preferential depopulation of the anti conformer through the formation of complexes with water present in the preexpansion gas mixture. The nearby aromatic group could hinder solvation of the folded, gauche conformation. The discrepancy in the two-color R2PI spectrum is enhanced by the different vertical ionization potentials of the anti (71 727-cm^{-1}) and gauche (71 039-cm^{-1}) conformers. These are in qualitative agreement with the values predicted by the ab initio calculations, 71 531 cm^{-1} (anti) and 70 699 cm^{-1} (gauche). Clearly, interpretation of the relative intensities in terms of conformer stabilities should be approached with some caution.

The experimental analyses that have been described have answered several old questions and have pointed the way to addressing many new ones. Rotational band contour analysis of the electronic spectra of individual molecular conformers isolated in the environment of a supersonic jet expansion is firmly established as a powerful probe of conformational choice and structure. The experiments have exposed a peculiar sensitivity of the polarization of an aromatic $\pi \rightarrow \pi^*$ transition to interactions with a folded, flexible chain substituent. Similar behavior has been observed in phenyl ethyl alcohol and phenyl propyl alcohol, where OH replaces COOH as the terminal polar end group.[4b] The interaction with the folded side chain provides a new and sensitive "conformational diagnostic", since its influence greatly amplifies the spectral consequences of conformational change and is clearly displayed, even when the rotational band contour is only partially resolved. The sensitivity of the transition polarization to the interaction with the side chain is the more remarkable when set against the very small spectral shift conferred by the side-chain substituent. The new diagnostic should encourage further exploitation of jet-cooled FE and REMPI spectroscopy in molecular conformational analysis and its further extension to higher resolution.[4c,d]

IV.B. Water Clusters. The results for the PPA$(H_2O)_{n=1,2}$ complexes provide answers to two fundamental questions: (1) where does the water bind, and (2) is the conformation modified significantly by the addition of water molecules? The simple answers from the present study are (1), firstly, as a proton acceptor from the carboxylic hydrogen and, secondly, as a proton acceptor from the first water adduct and a proton donor to the carbonyl oxygen to generate an overall cyclic structure, and (2) a qualified no. At the level of resolution attainable in the present study, the conformational integrity of the host molecule is preserved in the case of the anti conformer and broadly preserved in the case of the gauche conformer. The band contour for the 1:1 gauche complex shows little resolved structure, but assuming the water molecule again acts as a proton acceptor allows a reasonable fit to the experimental spectrum. The binding pattern, at least for the first water molecule, parallels the behavior found by Connell for indole−propionic acid.[5b] The 1:2 gauche complex is blue shifted, in marked contrast to the corresponding anti complex where a further small incremental red shift was recorded. We note, in this context, that the binding of water to benzene shifts the $6a^1_0$ band 40 cm^{-1} toward the blue.[10b] If the 1:2 gauche complex also adopts a cyclic structure, it would be possible for the second water molecule to interact with the aromatic ring.

A number of lessons have been learned (or relearned) from the sensitivity analysis of the band contour simulations. The position of a bound water molecule at the end of an extended side chain can exert a significant influence on the inertial properties of the molecular complex and thereby its rotational band contour, despite the small increment in the total mass. Thus, in the anti-PPA$-(H_2O)_{n=1}$ complex, where the H_2O molecule binds close to the *a* inertial axis but far from the *b* axis, the difference in inertial constants ($A'' - \bar{B}''$) increases, resulting in an, initially counterintuitive, increase in the spacing of the K_a subband heads. By the same token, the spectral contours were very sensitive to movement of the bound H_2O

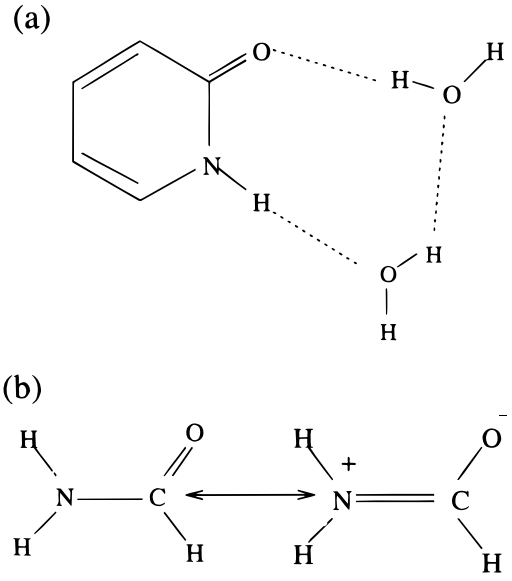

Figure 11. (a) Structure of the 2-pyridone−$(H_2O)_2$ complex from ref 19 and (b) a possible zwitterionic structure for the amide consistent with hydration-mediated geometry changes observed in 2-pyridone, *cf.* ref 19.

molecule in directions perpendicular to the *a* axis but relatively insensitive to movements parallel to it. This behavior emphasizes some of the limitations as well as the strengths of spectral simulations using partially resolved band contours.

The results do not provide answers to two further questions: (3) is there selectivity in the binding of water molecules to different conformers and/or to different binding sites (e.g., in HPPA), and (4) is the host molecular electronic structure modified by the bound water molecules? Question 3 has not been addressed in the present work. Question 4 can only be addressed through the analysis of excitation spectra recorded at much higher resolution. At this point, it is pertinent to review Held and Pratt's high-resolution study of the water complexes with the cyclic amide 2-pyridone, (2-PY), in particular 2-PY-$(H_2O)_{n=2}$.[19a] The cyclic structure of the $(H_2O)_{n=2}$ complex (shown in Figure 11a) is very similar to the structure proposed here, for the $n = 2$ complex with anti-PPA (see Figure 2b). More importantly however, Held and Pratt were able to determine the change in the structure of the host molecule, 2-PY, upon hydration by a single water molecule, namely, a reduction in the C−N and an increase in the C−O bond lengths, clearly reflecting a contribution from the zwitterionic structure shown in Figure 11b. There is a close analogy between the amide and carboxylate groups. Parallel high-resolution experiments on the water complexes of carboxylic acids such as PPA are planned to explore their approach to ionization—in effect, "pretransition state" spectroscopy for acid−base equilibrium.

Acknowledgment. This research was funded under a grant from the EPSRC. We thank the Laser Support Facility (LSF) at the Rutherford Appleton Laboratory (RAL) for the use of the GCR-11/PDL-3 laser system critical to the two-color R2PI experiments. J.P.S. thanks Monbuso for funding to enable collaboration with Prof. Okitsugu Kajimoto at Kyoto University and to allow J.A.D. to work in Kyoto and Ms. Seonkyung Lee to work in Oxford recording FE rovibronic band contours of the PPA monomer. We are especially grateful to Dr. Romano Kroemer for conducting a series of high level ab initio calculations on PPA and to Prof. David Pratt (University of Pittsburgh) for his advice, guidance, and judgement. P.W.J. thanks the Violette and Samuel Glasstone committee for fellowship support during this research. J.A.D. has been supported by an EPSRC CASE studentship in collaboration with the LSF at RAL.

References and Notes

(1) (a) Rizzo, T. R.; Levy, D. H. In Lasers and Mass Spectroscopy; Lubman, D. M., Ed.; Oxford University: Oxford, 1990; p 402 and references therein; (b) Rizzo, T. R.; Park, Y. D.; Peteanu, L.; Levy, D. H. *J. Chem. Phys.* **1986**, *84*, 2534. (c) Rizzo, T. R.; Park, Y. D.; Levy, D. H. *J. Chem. Phys.* **1986**, *85*, 6945. (d) Rizzo, T. R.; Park, Y. D.; Peteanu, L.; Levy, D. H. *J. Chem. Phys.* **1985**, *83*, 4819. (e) Park, Y. D.; Rizzo, T. R.; Peteanu, L.; Levy, D. H. *J. Chem. Phys.* **1986**, *84*, 6539. (f) Phillips, L. A.; Levy, D. H. *J. Chem. Phys.* **1986**, *85*, 1327. (g) Phillips, L. A.; Levy, D. H. *J. Chem. Phys.* **1986**, *90*, 4921.

(2) (a) Martinez, S. J.; Alfano, J. C.; Levy, D. H. *J. Mol. Spectrosc.* **1991**, *145*, 100. (b) Martinez, S. J.; Alfano, J. C.; Levy, D. H. *J. Mol. Spectrosc.* **1992**, *156*, 421. (c) Martinez, S. J.; Alfano, J. C.; Levy, D. H. *J. Mol. Spectrosc.* **1993**, *158*, 82.

(3) (a) Sipior, J.; Sulkes, M. *J. Chem. Phys.* **1993**, *98*, 9389. (b) Teh, C. K.; Sulkes, M. *J. Chem. Phys.* **1991**, *94*, 5826. (c) Sipior, J.; Sulkes, M. *J. Chem. Phys.* **1988**, *88*, 6146.

(4) (a) Howells, B. D.; McCombie, J.; Palmer, T. F.; Simons, J. P.; Waters, A. *J. Chem. Soc., Faraday Trans.* **1992**, *88*, 2587. (b) Walker, M. A. Ph.D. Thesis, Nottingham University, 1995. (c) Hepworth, P. A.; McCombie, J.; Simons, J. P.; Pfanstiel, J. F.; Ribblett, J. W.; Pratt, D. W. *Chem. Phys. Lett.* **1995**, *236*, 571. (d) Hepworth, P. A.; McCombie, J.; Simons, J. P.; Pfanstiel, J. F.; Ribblett, J. W.; Pratt, D. W. *Chem. Phys. Lett.* **1996**, *249*, 341.

(5) (a) Connell, L. L.; Corcoran, T. C.; Joireman, P. W.; Felker, P. M. *Chem. Phys. Lett.* **1990**, *166*, 510. (b) Connell, L. L. Ph.D. Thesis, University of California, Los Angeles, 1991.

(6) (a) Breen, P. J.; Warren, J. A.; Bernstein, E. R. *J. Chem. Phys.* **1987**, *87*, 1919. (b) Breen, P. J.; Warren, J. A.; Bernstein, E. R. *J. Chem. Phys.* **1987**, *87*, 1927. (c) Breen, P. J.; Bernstein, E. R.; Seeman, J. I. *J. Chem. Phys.* **1987**, *87*, 3269. (d) Breen, P. J.; Bernstein, E. R.; Secor, H. V.; Seeman, J. I. *J. Am. Chem. Soc.* **1989**, *111*, 1958. (e) Breen, P. J.; Warren, J. A.; Bernstein, E. R.; Seeman, J. I. *J. Am. Chem. Soc.* **1987**, *109*, 3453.

(7) (a) Ito, M.; Oikawa, A. *J. Mol. Struct.* **1985**, *126*, 133. (b) Yamamoto, S.; Okuyama, K.; Mikami, N.; Ito, M. *Chem. Phys. Lett.* **1986**, *125*, 1. (c) Ito, M. *J. Mol. Struct.* **1988**, *177*, 173. (d) Ito, M.; Yamamoto, S.; Aota, T.; Ebata, T. *J. Mol. Struct.* **1990**, *237*, 105. (e) Yamamoto, S.; Hashimoto, N.; Ito, M. *Bull. Chem. Soc. Jpn.* **1991**, *64*, 2202.

(8) Bellenger, P. A.; Dickinson, J. A.; Fujiwara, T.; Simons, J. P. To be submitted.

(9) Lubman, D. M.; Jordan, R. M. *Rev. Sci. Instrum.* **1985**, *56*, 373.

(10) (a) Gotch, A. J.; Garrett, A. W.; Severance, D. L.; Zwier, T. S. *Chem. Phys. Lett.* **1991**, *178*, 121. (b) Gotch, A. J.; Zwier, T. S. *J. Chem. Phys.* **1992**, *96*, 3388.

(11) Okabe, N.; Suga, T. *Acta. Crystalallogr. C* **1995**, *51*, 1324.

(12) Godfrey, P. D.; Hatherley, L. D.; Brown, R. D. *J. Am. Chem. Soc.* **1995**, *117*, 8204.

(13) Amir-Ebrahimi, V.; Choplin, A.; Demaison, J.; Roussy, G. *J. Mol. Spectrosc.* **1981**, *89*, 42.

(14) Caminati, W.; Damiani, D.; Corbelli, G.; Velino, B.; Bock, C. W. *Mol. Phys.* **1991**, *74*, 885.

(15) Callomon, J. H.; Dunn, T. M.; Mills, I. M. *Phil. Trans. R. Soc.* **1966**, *A259*, 449.

(16) (a) Bacon, A. R.; Hollas, J. M. *Faraday Discuss. Chem. Soc.* **1988**, *86*, 129. (b) Abe, H.; Mikami, N.; Ito, M. *J. Phys. Chem.* **1982**. *86*, 1768.

(17) Laser-induced fluorescence excitation spectra taken in our laboratory for this system under similar conditions exhibit intensity patterns consistent with our assignments. The intensity of the bands we assign to HPPA$(H_2O)_1$ are most intense relative to the monomer bands, followed by the peaks assigned to HPPA$(H_2O)_2$, as expected, given the relative populations of each species in the molecular beam.

(18) Nagy, P. I.; Smith, D. A.; Alagona, G.; Ghio, C. *J. Phys. Chem.* **1994**, *98*, 486.

(19) (a) Held, A; Pratt, D. W. *J. Am. Chem. Soc.* **1993**, *115*, 9708. (b) Held, A; Pratt, D. W. *J. Am. Chem. Soc.* **1993**, *115*, 9718.

(20) These calculations were performed by Dr. Romano Kroemer and detailed in: Joireman, P. W.; Kroemer, R.; Pratt, D. W.; Simons, J. P. *J. Chem. Phys.* **1996**, *105*, 6075. They involved a full geometry optimization using 6-31G* basis set and the Gaussian 94 package. Frisch, M. J.; Trucks, G. W.; Schlegel, H. B.; Gill, P. M. W.; Johnson, B. G.; Robb, M. A.; Cheeseman, J. R.; Keith, T.; Petersson, G. A.; Montgomery, J. A.; Raghavachari, K.; Al-Laham, M. A.; Zakrzewski, V. G.; Ortiz, J. V.; Foresman, J. B.; Cioslowski, J.; Stefanov, B. B.; Nanayakkara, A.; Challacombe, M.; Peng, C. Y.; Ayala, P. Y.; Chen, W.; Wong, M. W.; Andres, J. L.; Replogle, E. S.; Gomperts, R.; Martin, R. L.; Fox, D. J.; Binkley, J. S.; Defrees, D. J.; Baker, J.; Stewart, J. P.; Head-Gordon, M.; Gonzalez, C.; Pople, J. A. Gaussian 94, Revision C.3; Gaussian, Inc.: Pittsburgh, PA, 1995.